NANO LETTERS

Letter

pubs.acs.org/NanoLett

Selective-Area Fluorination of Graphene with Fluoropolymer and Laser Irradiation

Wi Hyoung Lee,[†,§] Ji Won Suk,[†] Harry Chou,[†] Jongho Lee,[‡] Yufeng Hao,[†] Yaping Wu,[†] Richard Piner,[†] Deji Akinwande,[‡] Kwang S. Kim,[§] and Rodney S. Ruoff*[,†]

[†]Department of Mechanical Engineering and the Materials Science and Engineering Program and [‡]Department of Electrical and Computer Engineering, Microelectronics Research Center, The University of Texas at Austin, Austin, Texas 78712, United States

[§]Center for Superfunctional Materials, Department of Chemistry, Pohang University of Science and Technology, Pohang 790-784, Korea

S *Supporting Information*

ABSTRACT: We have devised a method to selectively fluorinate graphene by irradiating fluoropolymer-covered graphene with a laser. This fluoropolymer produces active fluorine radicals under laser irradiation that react with graphene but only in the laser-irradiated region. The kinetics of C−F bond formation is dependent on both the laser power and fluoropolymer thickness, proving that fluorination occurs by the decomposition of the fluoropolymer. Fluorination leads to a dramatic increase in the resistance of the graphene while the basic skeletal structure of the carbon bonding network is maintained. Considering the simplicity of the fluorination process and that it allows patterning with a nontoxic fluoropolymer as a solid source, this method could find application to generate fluorinated graphene in graphene-based electronic devices such as for the electrical isolation of graphene.

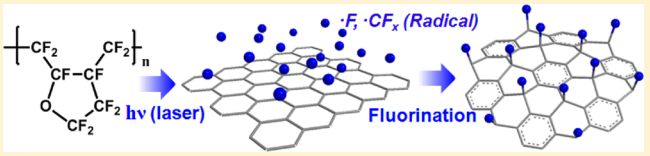

KEYWORDS: *Graphene, fluorinated graphene, graphene transfer, nanopatterning, laser irradiation*

Functionalized graphene has received considerable attention because it can change the chemical, structural, and electronic properties of graphene.[1−9] For example, graphene oxide is one of the most extensively studied forms of functionalized graphene and readily available by exfoliating oxidized graphite. However, the extensive oxidation can lead to fragmentation into smaller fragments and it is known that the oxidation is aperiodic.[4] In addition to epoxy and hydroxyl groups, other forms of functional groups are known to attach to the graphene basal plane and edge.[5,10] On the other hand, oxidation of pristine graphene produces different binding states of oxygen such as endoperoxide or charge-transfer complexes on the graphene, which suggests that oxidized forms of graphene are complicated and difficult to control.[11]

Hydrogenation or halogenation of graphene provides another possibility to tune the chemical functionalization of graphene such as for bandgap engineering.[12−24] Hydrogen plasma was used to make hydrogenated graphene and its structural and electrical properties were quite different from those of pristine graphene.[14,18,22] Halogenation has significant advantages over hydrogenation: (1) the high electronegativity of halogen atoms enables efficient doping and/or bandgap opening of the graphene and (2) fluorination, chlorination, or bromination can be applied to the graphene. Except for the exfoliation route to obtain fluorinated graphene from graphite fluoride,[23,24] gaseous species have been commonly used to synthesize halogenated graphene.[15−17,19,21,22] F or Cl plasma, or F_2 exposure at high temperature, have been used to attach F or Cl atoms to the basal plane of graphene.[15,22] However, plasma can damage the graphene by ion bombardment and high-temperature reactions are not recommended.[17,25] Decomposition of XeF_2 at low temperature or photochemical decomposition of Cl_2 was also demonstrated for the fluorination or chlorination of graphene.[16,17,19,21] An environmentally friendly and nontoxic process that enables efficient and controllable halogenations is thus a valuable target goal.

The controlled fluorination of graphene by using a solid fluorine source and laser irradiation is reported here. The fluoropolymer, CYTOP (Cytop, CTL-809 M from Asahi Glass Co.) was used as a solid source and a Raman laser (WITec alpha300, λ_{laser} = 488 nm, ∼500 nm spot size) was used to decompose the CYTOP for the formation of the fluorine precursor. Chemical vapor deposition (CVD)-grown large-area graphene on Cu foil was used for study of fluorination with CYTOP. Selective (patterned) fluorination of the graphene was achieved, which is highly favorable for the integration of fluorinated graphene into functional devices.

As-synthesized monolayer graphene film on Cu foil was transferred onto a SiO_2 (thickness of 285 nm)/Si substrate by a polymer-assisted transfer method.[26−29] We used CYTOP to transfer the graphene and avoided trapping residual polymethylmethacrylate (PMMA) between the CYTOP and graphene, thus achieving direct contact between CYTOP and

Received: January 26, 2012
Revised: March 30, 2012
Published: April 6, 2012

   dx.doi.org/10.1021/nl300346j | *Nano Lett.* 2012, 12, 2374−2378

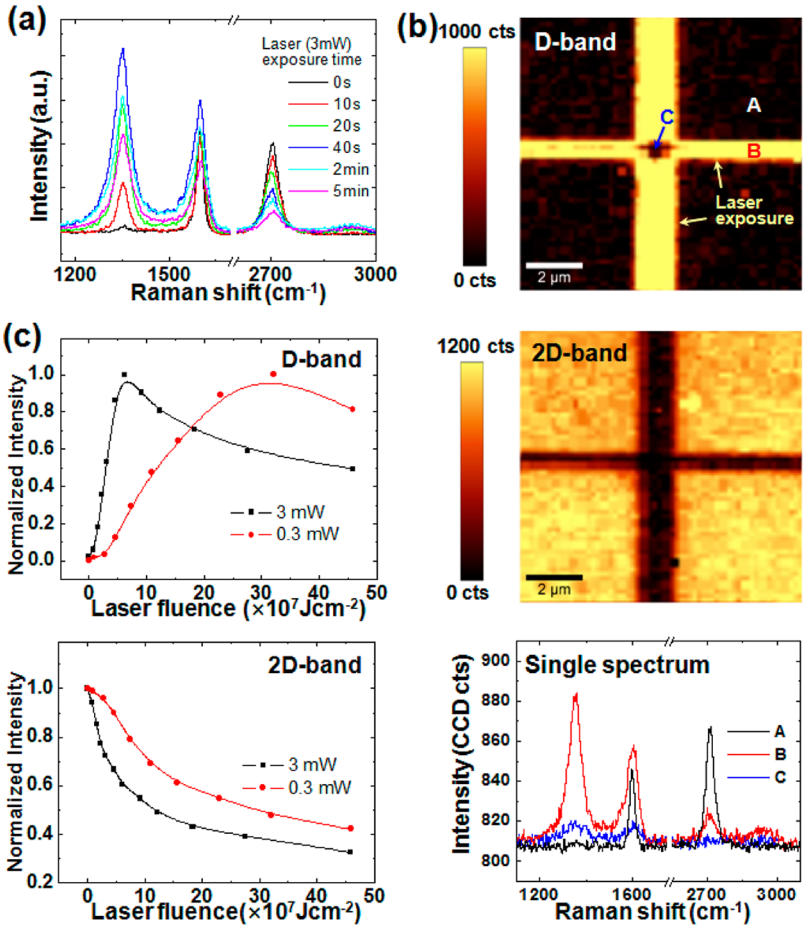

Figure 1. (a) Change of the Raman spectrum of the CYTOP-covered graphene film as a function of laser irradiation time (0, 10, 20, 40 s; 2 and 5 min). The graphene film was transferred by CYTOP (~15 nm) and then was selectively irradiated with a Raman laser (WITec alpha300, λ_{laser} = 488 nm, ~500 nm spot size, 100× objective lens, laser power: 3 mW). (b) Raman maps of the D- (1300−1500 cm^{-1}), and 2D- (2600−2800 cm^{-1}) bands, respectively. Bottom plots show single spectra from the marked A, B, and C spots. The defects of graphene, which are spaced within the selected-area, were formed by irradiating CYTOP-covered graphene with the laser (power: 10 mW). Raman scanning (power: 0.3 mW) was used to obtain the maps. (c) Plots for the intensities of D- and 2D-bands as a function of the laser fluence. The D-band intensities were normalized by the maximum intensity whereas the 2D-band intensities were normalized by the initial intensity before laser irradiation (Black rectangles, 3 mW laser power; red circles, 0.3 mW laser power).

the graphene surface. Figure 1a shows the change in the Raman spectrum of CYTOP (thickness of 15 nm)-covered graphene as a function of laser irradiation time. The intensity of the D band at 1350 cm^{-1}, which was negligible before laser irradiation, increases sharply as laser irradiation time increases (0−40 s). On the other hand, the intensity of the 2D band at 2700 cm^{-1} decreases gradually. These results indicate a breaking of the translational symmetry of the sp^2 bonded network in graphene with laser irradiation.[16,17] When the laser irradiation time is increased even more, the intensities of D-, G-, and 2D-band decrease at the same time and a new band at 2940 cm^{-1} appears. This new band corresponds to a combination mode of the D- and G-bands, which was observed in fluorinated graphene.[16,17] The regions of fluorination in graphene can be patterned by positioning the laser. Raman scanning (laser power: 10 mW), which is routinely used for characterizing the quality of graphene, is used here to produce structural disorder (i.e., top fluorinate) in a defined area. Afterward, a Raman map with a low laser power (0.3 mW) was obtained to characterize the irradiated graphene film. Figure 1b shows Raman maps of the D- and 2D-bands of the graphene film and a single spectra from the marked A, B, and C spots. The D-band is only detected at the cross pattern where the laser passed through. On the other hand, the 2D-band exhibits the opposite trend. Interestingly, both the D- and 2D-bands are relatively small at the center of the cross pattern at which laser irradiation time is the highest. This corresponds well with the time dependent change of the Raman spectrum as shown in Figure 1a and can be interpreted as enhanced structural disorder in a local active model of the D-band.[18,30] According to this model, intensity of the D-band decreases gradually by an overlapping of the activation areas in the disordered regions notwithstanding an overall increase of structural disorder in the graphene.

To examine the relationship between laser power and the structural disorder induced within graphene, a laser with two different powers (0.3 and 3 mW) was used to irradiate graphene films and the relative intensity changes in the D-band and 2D-band were plotted in Figure 1c. A low laser power, 0.3 mW, gave a reduced peak change rate compared to power of 3 mW (compare Figure 1a and Supporting Information Figure S1). Although the 3 mW laser power exhibits a higher overall rate of change, the 0.3 and 3 mW laser power show similar trends in peak intensity changes: (1) a slow change in D- and 2D-band intensities at the initial stage, (2) an abrupt change in

dx.doi.org/10.1021/nl300346j | Nano Lett. 2012, 12, 2374−2378

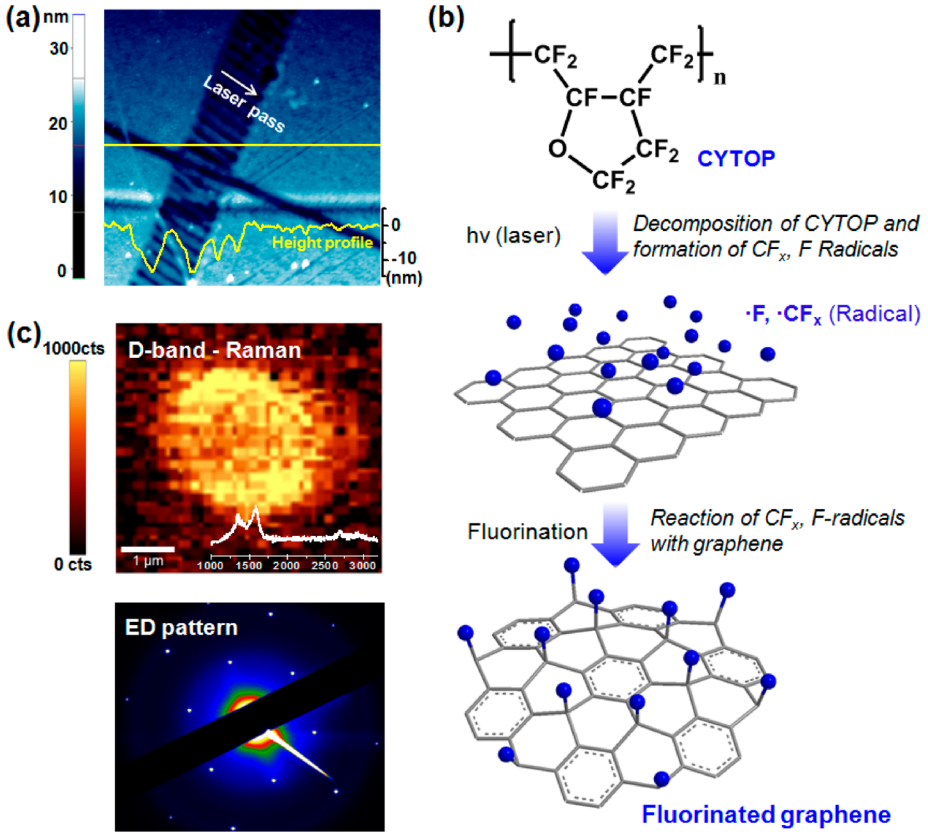

Figure 2. (a) AFM image and height profile of the CYTOP-covered graphene after selective-area laser exposure. The exposure condition is the same as in Figure 1b. (b) The scheme showing a mechanism for fluorination by using CYTOP and laser irradiation. (c) (Top) Raman map (D-band: from 1300 to 1450 cm^{-1}) of the fluorinated graphene film adhered to a SiN_x membrane (with hole diameter of 3 μm). Inset shows a single spectrum of a freestanding graphene film after fluorination. (Bottom) Typical selected-area electron diffraction pattern of the fluorinated graphene membrane.

peak intensities at an intermediate stage, (3) and a decrease and saturation at a minimum value of the peak intensity at the final stage. The amount of disorder induced in graphene is thus affected by both the laser power and the irradiation time. Furthermore, when a thinner CYTOP layer (~2 nm) was used instead, the yield was greatly reduced (see Supporting Information Figure S2). These results strongly imply that irradiation-induced structural disorder does not follow a single-photon process as in the photochemical reaction of graphene and that the phenomena might be due, instead, to active intermediates.[31]

To better understand the structural disorder phenomena, a surface profile of the CYTOP-covered graphene after laser patterning was examined by atomic force microscopy (AFM) (Figure 2a). The AFM image shows that the grooves correlate with laser irradiation, confirming selective removal of CYTOP by laser irradiation. Thus, it is reasonable to speculate that the structural disorder in graphene is closely related to the decomposition of CYTOP. We surmise that the light source with high photon flux induces a chain scission reaction and defluorination of the backbone of this fluoropolymer.[32−34] Additionally, we expect that heat generation has little effect on structural disorder in graphene. This is supported by noting that (i) heat may dissipate through the substrate, (ii) the 2D-band does not show a temperature-induced shift,[35,36] (iii) the D-band was detected after exposure to even low laser power (20 μW) (see Supporting Information Figure S3) where heat generation is negligible, (iv) and thermal annealing at 250 and 450 °C does not create as much structural disorder as irradiation does (see Supporting Information Figure S4). Laser-induced decomposition of CYTOP will produce many active intermediates such as CF_x and F radicals, as well as char.[34] These CF_x and F radicals can react with sp^2-hybrized graphene and form a C−F sp^3 bond. In a control experiment to examine correlation between CYTOP and the structural disorder within graphene, the graphene film was transferred by PMMA and then irradiated with a Raman laser. Even after long exposure time to laser, D-band was not detected (see Supporting Information Figure S5). This result confirms that laser irradiation of graphene without CYTOP layer does not induce any structural disorder within graphene and decomposition of CYTOP under laser irradiation is the main reason for the observed phenomena. Figure 2b shows a schematic representation of our fluorination process using CYTOP and laser irradiation. Because active fluorine species are present only on one side of the graphene and because the active fluorine species cannot permeate through to the SiO_2/Si substrate,[16,17] we obtain single-side fluorinated graphene (or partially fluorinated graphene) with this process. Oxygen molecules in the atmosphere could also possibly contribute to the structural disorder. However, oxidation of graphene only contributes to a relatively small increase in the D-band intensity and only occurs in a high-temperature reaction, thereby ruling out this possibility.[11] With this process, we can conclude that the laser irradiation both causes decomposition of CYTOP and facilitates patterned fluorination in the underlying graphene.

To evaluate the structural properties of fluorinated graphene, CVD-grown graphene was transferred onto a SiN_x membrane

dx.doi.org/10.1021/nl300346j | Nano Lett. 2012, 12, 2374−2378

using CYTOP, followed by laser irradiation. Figure 2c top shows the D-band (1200−1450 cm^{-1}) map of fluorinated graphene on a SiN_x membrane. Because there are indicators from the graphene placed on the SiN_x, the freestanding regions can be easily detected from the map.[29] A single spectrum of the graphene membrane exhibits D- and G-bands with a similar intensity ratio, as well as a negligible 2D-band (Figure 2c top inset). The electron diffraction pattern from transmission electron microscopy (TEM, FEI Titan S operating at 80 keV) confirms that our fluorinated graphene maintains the basic skeletal structure of the carbon binding network, and is similar in quality to that of pristine graphene (see Supporting Information Figure S6) and fluorinated graphene from other groups.[17,19,24] Recent theoretical calculations predict that partially fluorinated graphene is structurally stable and the atomic and electronic structures are dependent on the coverage of fluorine atoms.[12,37,38] The 25% coverage (C_4F), which is known to be the lowest energy configuration in single-side fluorinated graphene,[16,37] is a possible stoichiometry for this process, but we are not able to confirm that at this stage. In a control experiment to determine the size of the attached fluorine species, the graphene film was transferred by PMMA, covered by CYTOP (~15 nm), and then selectively irradiated with a Raman laser. Although the CYTOP layer contacts an ultrathin (thickness of 1−2 nm) PMMA residue rather than the graphene surface,[39,40] the amount of structural disorder is not less than that of CYTOP-transferred graphene (see Supporting Information Figure S7). This suggests that PMMA residue does not limit the kinetics of fluorination. Thus active fluorine species are CF_x/F radicals, and predominantly F radicals, and not radicals with long chains because long chains cannot permeate through PMMA residue and form bonds with the sp^2-hybrized graphene.

To examine the change in electrical properties with fluorination, Ti (5 nm)/Au (30 nm) source/drain electrodes were deposited on the graphene after defining patterns using standard e-beam lithography (Figure 3a inset). Raman spectra and electrical properties were measured after device fabrication. The device was covered by CYTOP and the channel region was selectively fluorinated by exposure with a Raman laser (following the same procedure in Supporting Information Figure S7). Figure 3a,b shows Raman spectra of the graphene film in the channel region and current−voltage characteristics of the graphene device, respectively. We checked two different fluorination stages: at the point where the D-band is high (fluorination stage1) and at the point where the decreases of the D- and 2D-bands are saturated and the 2D-band is negligibly small (fluorination stage2). Note that the degree of fluorination is higher at the latter point.[17] After fluorination stage1, the resistance increases by around 2 orders of magnitude (from 4.8 kΩ to 0.43 MΩ). Further fluorination (fluorination stage2) leads to an abrupt increase in resistance of >10 GΩ, which is nearly the resolution limit of our semiconductor parameter analyzer setup. This highly insulating behavior corresponds well with experimental results on the fluorinated graphene synthesized from XeF_2 or exfoliated from graphite fluoride.[16,17,24] Although the fluorinated graphene synthesized in our method is not "fluorographene" (stoichiometry CF) since it is graphene fluorinated only on one side (C_nF, n greater than 1), its bandgap should be large enough to be considered an insulator.[16,38]

In conclusion, graphene has been selectively fluorinated by irradiating fluoropolymer-covered graphene with a laser. The active fluorine radicals produced by photon-induced decomposition of the fluoropolymer react with the sp^2-hybrized graphene, and form C−F bonds. This fluorinated graphene exhibited nearly the same structural and electrical properties as those of single-side fluorinated graphene synthesized from XeF_2 and exfoliated graphite fluoride. This is an efficient method for isolating graphene devices because the laser irradiation on fluoropolymer-covered graphene process produces fluorinated graphene with highly insulating properties in a single step. This will reduce production costs by circumventing the complicated isolation patterning procedures such as photolithography, etching, and lift off.

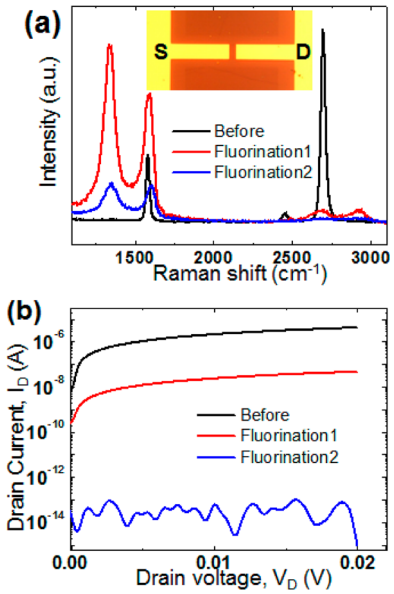

Figure 3. (a) Change of the Raman spectrum in the channel region of the graphene devices before and after fluorination. Inset shows the image of the graphene devices with a channel length of 2 μm and width of 5 μm. Raman mapping was used to fluorinate the channel region of the graphene devices. (b) Change of the current−voltage characteristics of the graphene devices before and after fluorination. The source−drain voltage (V_D) was swept from 0 to 0.02 V at zero gate voltage.

■ ASSOCIATED CONTENT

Supporting Information

Figures S1−S7. This material is available free of charge via the Internet at http://pubs.acs.org.

■ AUTHOR INFORMATION

Corresponding Author

*E-mail: r.ruoff@mail.utexas.edu.

Notes

The authors declare no competing financial interest.

■ ACKNOWLEDGMENTS

This research was supported by the National Science Foundation Award No. 1006350, the Office of Naval Research, the Nanoelectronic Research Initiative (NRI SWAN Center), as well as from the NRF of Korea (National Honor Scientist Program: 2010-0020414, partial support of WHL).

REFERENCES

(1) Zhu, Y. W.; Murali, S.; Cai, W. W.; Li, X. S.; Suk, J. W.; Potts, J. R.; Ruoff, R. S. *Adv. Mater.* **2010**, *22* (46), 5226−5226.
(2) Rao, C. N. R.; Sood, A. K.; Subrahmanyam, K. S.; Govindaraj, A. *Angew. Chem., Int. Ed.* **2009**, *48* (42), 7752−7777.
(3) Dreyer, D. R.; Ruoff, R. S.; Bielawski, C. W. *Angew. Chem., Int. Ed.* **2010**, *49* (49), 9336−9344.
(4) Park, S.; Ruoff, R. S. *Nat. Nanotechnol.* **2009**, *4* (4), 217−224.
(5) Loh, K. P.; Bao, Q. L.; Eda, G.; Chhowalla, M. *Nature Chem.* **2010**, *2* (12), 1015−1024.
(6) Eda, G.; Chhowalla, M. *Adv. Mater.* **2010**, *22* (22), 2392−2415.
(7) Lee, S. H.; Lee, D. H.; Lee, W. J.; Kim, S. O. *Adv. Funct. Mater.* **2011**, *21* (8), 1338−1354.
(8) Yan, L.; Zheng, Y. B.; Zhao, F.; Li, S. J.; Gao, X. F.; Xu, B. Q.; Weiss, P. S.; Zhao, Y. L. *Chem. Soc. Rev.* **2012**, *41* (1), 97−114.
(9) Geim, A. K. *Science* **2009**, *324* (5934), 1530−1534.
(10) Gao, W.; Alemany, L. B.; Ci, L. J.; Ajayan, P. M. *Nature Chem.* **2009**, *1* (5), 403−408.
(11) Liu, L.; Ryu, S. M.; Tomasik, M. R.; Stolyarova, E.; Jung, N.; Hybertsen, M. S.; Steigerwald, M. L.; Brus, L. E.; Flynn, G. W. *Nano Lett.* **2008**, *8* (7), 1965−1970.
(12) Sofo, J. O.; Chaudhari, A. S.; Barber, G. D. *Phys. Rev. B* **2007**, *75* (15), 153401.
(13) Ryu, S.; Han, M. Y.; Maultzsch, J.; Heinz, T. F.; Kim, P.; Steigerwald, M. L.; Brus, L. E. *Nano Lett.* **2008**, *8* (12), 4597−4602.
(14) Elias, D. C.; Nair, R. R.; Mohiuddin, T. M. G.; Morozov, S. V.; Blake, P.; Halsall, M. P.; Ferrari, A. C.; Boukhvalov, D. W.; Katsnelson, M. I.; Geim, A. K.; Novoselov, K. S. *Science* **2009**, *323* (5914), 610−613.
(15) Withers, F.; Dubois, M.; Savchenko, A. K. *Phys. Rev. B* **2010**, *82* (7), 073403.
(16) Robinson, J. T.; Burgess, J. S.; Junkermeier, C. E.; Badescu, S. C.; Reinecke, T. L.; Perkins, F. K.; Zalalutdniov, M. K.; Baldwin, J. W.; Culbertson, J. C.; Sheehan, P. E.; Snow, E. S. *Nano Lett.* **2010**, *10* (8), 3001−3005.
(17) Nair, R. R.; Ren, W. C.; Jalil, R.; Riaz, I.; Kravets, V. G.; Britnell, L.; Blake, P.; Schedin, F.; Mayorov, A. S.; Yuan, S. J.; Katsnelson, M. I.; Cheng, H. M.; Strupinski, W.; Bulusheva, L. G.; Okotrub, A. V.; Grigorieva, I. V.; Grigorenko, A. N.; Novoselov, K. S.; Geim, A. K. *Small* **2010**, *6* (24), 2877−2884.
(18) Luo, Z. Q.; Yu, T.; Ni, Z. H.; Lim, S. H.; Hu, H. L.; Shang, J. Z.; Liu, L.; Shen, Z. X.; Lin, J. Y. *J. Phys. Chem. C* **2011**, *115* (5), 1422−1427.
(19) Jeon, K. J.; Lee, Z.; Pollak, E.; Moreschini, L.; Bostwick, A.; Park, C. M.; Mendelsberg, R.; Radmilovic, V.; Kostecki, R.; Richardson, T. J.; Rotenberg, E. *ACS Nano* **2011**, *5* (2), 1042−1046.
(20) Withers, F.; Bointon, T. H.; Dubois, M.; Russo, S.; Craciun, M. F. *Nano Lett.* **2011**, *11* (9), 3912−3916.
(21) Li, B.; Zhou, L.; Wu, D.; Peng, H. L.; Yan, K.; Zhou, Y.; Liu, Z. F. *ACS Nano* **2011**, *5* (7), 5957−5961.
(22) Wu, J.; Xie, L.; Li, Y.; Wang, H.; Ouyang, Y.; Guo, J.; Dai, H. *J. Am. Chem. Soc.* **2011**, *133* (49), 19668−71.
(23) Zboril, R.; Karlicky, F.; Bourlinos, A. B.; Steriotis, T. A.; Stubos, A. K.; Georgakilas, V.; Safarova, K.; Jancik, D.; Trapalis, C.; Otyepka, M. *Small* **2010**, *6* (24), 2885−2891.
(24) Cheng, S. H.; Zou, K.; Okino, F.; Gutierrez, H. R.; Gupta, A.; Shen, N.; Eklund, P. C.; Sofo, J. O.; Zhu, J. *Phys. Rev. B* **2010**, *81* (20), 205435.
(25) Yang, R.; Zhang, L. C.; Wang, Y.; Shi, Z. W.; Shi, D. X.; Gao, H. J.; Wang, E. G.; Zhang, G. Y. *Adv. Mater.* **2010**, *22* (36), 4014−4019.
(26) Li, X. S.; Cai, W. W.; An, J. H.; Kim, S.; Nah, J.; Yang, D. X.; Piner, R.; Velamakanni, A.; Jung, I.; Tutuc, E.; Banerjee, S. K.; Colombo, L.; Ruoff, R. S. *Science* **2009**, *324* (5932), 1312−1314.
(27) Li, X. S.; Zhu, Y. W.; Cai, W. W.; Borysiak, M.; Han, B. Y.; Chen, D.; Piner, R. D.; Colombo, L.; Ruoff, R. S. *Nano Lett.* **2009**, *9* (12), 4359−4363.
(28) Lee, Y.; Bae, S.; Jang, H.; Jang, S.; Zhu, S. E.; Sim, S. H.; Song, Y. I.; Hong, B. H.; Ahn, J. H. *Nano Lett.* **2010**, *10* (2), 490−493.
(29) Suk, J. W.; Kitt, A.; Magnuson, C. W.; Hao, Y. F.; Ahmed, S.; An, J. H.; Swan, A. K.; Goldberg, B. B.; Ruoff, R. S. *ACS Nano* **2011**, *5* (9), 6916−6924.
(30) Lucchese, M. M.; Stavale, F.; Ferreira, E. H. M.; Vilani, C.; Moutinho, M. V. O.; Capaz, R. B.; Achete, C. A.; Jorio, A. *Carbon* **2010**, *48* (5), 1592−1597.
(31) Liu, H. T.; Ryu, S. M.; Chen, Z. Y.; Steigerwald, M. L.; Nuckolls, C.; Brus, L. E. *J. Am. Chem. Soc.* **2009**, *131* (47), 17099−17101.
(32) French, R. H.; Wheland, R. C.; Qiu, W. M.; Lemon, M. F.; Zhang, E.; Gordon, J.; Petrov, V. A.; Cherstkov, V. F.; Delaygina, N. I. *J. Fluorine Chem.* **2003**, *122* (1), 63−80.
(33) Lee, K.; Jockusch, S.; Turro, N. J.; French, R. H.; Wheland, R. C.; Lemon, M. F.; Braun, A. M.; Widerschpan, T.; Dixon, D. A.; Li, J.; Ivan, M.; Zimmerman, P. *J. Am. Chem. Soc.* **2005**, *127* (23), 8320−8327.
(34) Blakey, I.; George, G. A.; Hill, D. J. T.; Liu, H. P.; Rasoul, F.; Rintoul, L.; Zimmerman, P.; Whittaker, A. K. *Macromolecules* **2007**, *40* (25), 8954−8961.
(35) Chen, S. S.; Moore, A. L.; Cai, W. W.; Suk, J. W.; An, J. H.; Mishra, C.; Amos, C.; Magnuson, C. W.; Kang, J. Y.; Shi, L.; Ruoff, R. S. *ACS Nano* **2011**, *5* (1), 321−328.
(36) Balandin, A. A. *Nat. Mater.* **2011**, *10* (8), 569−81.
(37) Xiang, H. J.; Kan, E. J.; Wei, S. H.; Gong, X. G.; Whangbo, M. H. *Phys. Rev. B* **2010**, *82* (16), 165425.
(38) Sahin, H.; Topsakal, M.; Ciraci, S. *Phys. Rev. B* **2011**, *83* (11), 115432.
(39) Dan, Y. P.; Lu, Y.; Kybert, N. J.; Luo, Z. T.; Johnson, A. T. C. *Nano Lett.* **2009**, *9* (4), 1472−1475.
(40) Lee, W. H.; Park, J.; Sim, S. H.; Lim, S.; Kim, K. S.; Hong, B. H.; Cho, K. *J. Am. Chem. Soc.* **2011**, *133* (12), 4447−4454.